LIMNOLOGY and OCEANOGRAPHY

ASLO

Limnol. Oceanogr. 68, 2023, S217–S229

doi: 10.1002/lno.12375

Ocean acidification altered microbial functional potential in the Arctic Ocean

Yu Wang[1], **Rui Zhang**[1,2], **Yunfeng Yang**[3], **Qichao Tu**[4], **Jizhong Zhou**[3,5,6*], **Nianzhi Jiao**[1*]

[1]State Key Laboratory of Marine Environmental Science, College of Ocean and Earth Sciences, College of Environment and Ecology, Fujian Key Laboratory of Marine Carbon Sequestration, Innovation Research Center for Carbon Neutralization, Xiamen University, Xiamen, Fujian, China
[2]Marine Science and Engineering Guangdong Laboratory (Zhuhai), Zhuhai, Guangdong, China
[3]State Key Laboratory of Environment Simulation and Pollution Control, School of Environment, Tsinghua University, Beijing, China
[4]Institute of Marine Science and Technology, Shandong University, Qingdao, Shandong, China
[5]Institute for Environmental Genomics and Department of Microbiology and Plant Biology, University of Oklahoma, Norman, Oklahoma, USA
[6]Earth and Environmental Sciences, Lawrence Berkeley National Laboratory, Berkeley, California, USA

Abstract

Ocean acidification (OA) has considerably changed the metabolism and structure of plankton communities in the ocean. Evaluation of the response of the marine bacterioplankton community to OA is critical for understanding the future direction of bacterioplankton-mediated biogeochemical processes in the ocean. Understanding the diversity of functional genes is important for linking the microbial community to ecological and biogeochemical processes. However, the influence of OA on the functional diversity of bacterioplankton remains unclear. Using high-throughput functional gene microarray technology (GeoChip 4), we investigated the functional gene structure and diversity of bacterioplankton under three different pCO_2 levels (control: 175 μatm, medium: 675 μatm, and high: 1085 μatm) in a large Arctic Ocean mesocosm experiment. We observed a higher evenness of microbial functional genes under elevated pCO_2 compared with under low pCO_2. OA induced a more stable community as evaluated by decreased dissimilarity of functional gene structure with increased pCO_2. Molecular ecological networks under elevated pCO_2 became more complex and stable, supporting the central ecological tenet that complexity begets stability. In particular, increased average abundances were found under elevated pCO_2 for many genes involved in key metabolic processes, including carbon degradation, methane oxidization, nitrogen fixation, dissimilatory nitrite/nitrate reduction, and sulfide reduction processes. Altogether, these results indicate a significant influence of OA on the metabolism potential of bacterioplankton in the Arctic Ocean. Consequently, our study suggests that biogeochemical cycling mediated by these microbes may be altered by the OA in the future.

*Correspondence: jiao@xmu.edu.cn, jzhou@ou.edu

Additional Supporting Information may be found in the online version of this article.

Yu Wang and Rui Zhang contribution equally to this study.

Author Contribution Statement: R.Z., J.Z., and N.J. contributed to the theoretical designs. R.Z. performed the sampling. Y.W. performed GeoChip experiment, and analyzed all data. Y.W. and R.Z. wrote the manuscript with the help of all authors. Y.Y. and Q.T. made a great contribution to the revision of the manuscript and the analysis of the additional data. All authors contributed to the final version of the manuscript.

Special Issue: Cascading, Interactive, and Indirect Effects of Climate Change on Aquatic Communities, Habitats, and Ecosystems. *Edited by: Susanne Menden-Deuer, Maarten Boersma, Hans-Peter Grossart, Ryan Sponseller, Sarah A. Woodin and Deputy Editors Julia C. Mullarney, Steeve Comeau, and Elisa Schaum.*

The oceans absorbed approximately 25% of the CO_2 produced by fossil fuel burning and cement production (Raven et al. 2005; Joint et al. 2011; Quéré et al. 2013). Without ocean uptake, the present level of atmospheric CO_2 would be approximately 450 ppm today (Doney et al. 2009). This phenomenon decreases the pH of the oceans, resulting in ocean acidification (OA). It is estimated that the average pH of the oceans has decreased by 0.1 units from 8.2 after the start of the industrial revolution (Raven et al. 2005) and is expected to decrease by 0.2–0.4 units by the year 2100 (Caldeira and Wickett 2005; IPCC 2015). Therefore, there is significant interest in how OA will affect the ocean's biota and integral processes (Cavicchioli et al. 2019). OA influences a wide range of marine biota across multiple trophic levels, such as phytoplankton (Dutkiewicz et al. 2015), coral reefs (Hofmann et al. 2010; Fantazzini et al. 2015; Zhou et al. 2016), and shellfish (Ekstrom et al. 2015). Numerous studies have indicated that OA may affect the structure of plankton communities and the biogeochemical cycling of elements (Newbold et al. 2012; Maas et al. 2013; Eberlein et al. 2017). For example, a study of the Ross Sea demonstrated that OA reduced bacterial diversity and enhanced the ability of phytoplankton to break down carbohydrates and lipids (Maas et al. 2013). In addition, picoeukaryote community structures were shifted by increasing CO_2 concentration (Newbold et al. 2012). Therefore, OA remains a critical issue for global marine ecosystems.

Bacterioplankton are ubiquitous in the ocean environment and are one of the major drivers of marine biogeochemical cycles (Falkowski et al. 1998; Whitman et al. 1998). Bacterioplankton utilizes up to half of the carbon fixed by phytoplankton, ~ 25 Pg C yr^{-1} (Azam et al. 1983). In addition to converting carbon into bacterial biomass and CO_2 by respiration, bacterioplankton transfer carbon either to higher trophic levels by predation or to the marine organic pool by viral lysis (Azam et al. 1983; Fuhrman 1999; Azam and Malfatti 2007). Microbial carbon pump theory emphasizes the importance of bacterioplankton in the transformation of labile dissolved organic carbon (DOC) into recalcitrant DOC (Jiao et al. 2010). Bacterioplankton also plays an important role in nitrogen cycling via processes such as nitrogen fixation (Turk-Kubo et al. 2014), nitrification (van Kessel et al. 2015), and denitrification (Ward et al. 2009). Previous studies have observed the changes in the activity of microbial communities by OA, including bacterial production (BP; Deppeler et al. 2018; Westwood et al. 2018), growth rate (Crawfurd et al. 2017), and the uptake of nutrients (Maas et al. 2013), factors that influence biogeochemical processes mediated by bacterioplankton. The function of microorganisms in ecological and biogeochemical processes depends on the activities or behaviors associated with their functional genes (Robinson et al. 2010). Also, the presence/absence and diversity of microbial functional genes indicate the presence of relevant functional potential in the ecosystem. Therefore, understanding the diversity of functional genes is important for bridging the microbial community to ecological and biogeochemical processes. In turn, the microbial community is inevitably influenced by the environment it inhabits. However, little is known about the influence of OA on the functional diversity of the bacterioplankton community. This knowledge gap hampers our understanding of the processes and mechanisms of marine biogeochemical cycling.

Polar oceans—such as the Arctic Ocean—are more susceptible to the impacts of OA in the near future due to the higher CO_2 solubility in colder water (Monier et al. 2014). The marine organisms and ecosystems in the Arctic are considered particularly vulnerable to OA (Riebesell et al. 2013). Under the European Project on Ocean Acidification (EPOCA) framework, a large-scale mesocosm experiment was conducted at Kongsfjorden, Ny-Ålesund, Svalbard using Kiel Off-Shore Mesocosms for Ocean Simulations to mimic the different pCO_2 scenarios. Nine pCO_2 manipulations of the EPOCA experiment were employed from ~ 160 to ~ 1085 μatm with 30-d incubation (nine pCO_2 levels). Each mesocosm contained approximately 50 m^3 in situ seawater. This was one of the largest scale mesocosm experiments performed for measuring the effects of OA to date (Quirin 2011; Riebesell et al. 2013), which provided an ideal system for simulating the conditions under which to investigate the response of the marine ecosystem to OA. The EPOCA Svalbard experiment has illustrated various responses of plankton scaled up to the community level (Riebesell et al. 2013). Previous studies from the EPOCA Svalbard experiment demonstrated that the phylogenetic structure and diversity of bacterioplankton communities did not in general respond clearly to elevated pCO_2 (Roy et al. 2013; Zhang et al. 2013). The abundance patterns of bacterioplankton and virioplankton increased during the experiment and were similar among the different pCO_2 treatments (Brussaard et al. 2013). However, bacterial protein production and extracellular enzymes of bacterioplankton were stimulated by elevated pCO_2 (Engel et al. 2013; Piontek et al. 2013). In addition, the elevated pCO_2 could alter the growth balance of bacteria as revealed by the leucine-to-thymidine incorporation ratio (Motegi et al. 2013). Therefore, there was a clear gap between the responses of microbial phylogenetic diversity and microbial community function to OA. To fill this gap, we employed a high-throughput functional gene microarray to investigate the functional gene structure and diversity of the bacterioplankton community under elevated pCO_2 from the EPOCA Svalbard experiment. In this study, we addressed the following questions: (1) whether the functional gene diversity and structure of the bacterioplankton community were impacted by the elevated pCO_2, and (2) which specific functions were altered. This study can reveal the importance of elucidating functional gene diversity and structure of the bacterioplankton community for enhancing our understanding of ecosystem responses to OA.

Materials and methods

Experimental setup and sampling

In the framework of EPOCA, pCO_2 manipulation mesocosms were set up in the coastal area near Kongsfjorden, northern Spitsbergen (78°56′2″N, 11°53′6″E) from June to July 2010 (Supporting Information Fig. S1). Detailed information about the setup of this experiment, pCO_2-perturbation of seawater within the mesocosm, and sampling procedures have been published (Czerny et al. 2013; Riebesell et al. 2013; Schulz et al. 2013). Briefly, nine units of the Kiel Off-Shore Mesocosms for Ocean Simulations (KOSMOS) with 30-d incubation were employed. Each KOMOS unit enclosed ca. 50 m^3 in situ seawater in a 17-m long, 2 m in diameter polyurethane bag. To reach the target pCO_2 level, the CO_2-saturated seawater was added to the mesocosms. Three representative mesocosms were selected with control (M3: 175 μatm), medium (M6: 675 μatm), and high (M9: 1085 μatm) pCO_2 concentrations. The three mesocosms indicated the pCO_2 level in the in situ environment (M3) and the level under the projected scenario for the year 2100 (M6) and beyond (M9), and thus extrapolations may be appropriate to ecosystems exhibiting similar levels of CO_2 system drivers (Bellerby et al. 2012). Samples for DNA extraction were collected on days −1 (the day before CO_2 addition), 1, 4, 7, 12, 14, 18, 20, 22, 26, 28, and 30 from each mesocosm during the experiment. A total of 36 samples were collected and stored at −80°C until the following extraction. Various chemical and biological variables were measured during the experiment, which can be found on the EPOCA website (http://www.epoca-project.eu). In this study, environmental variables, including pCO_2, pH, salinity, temperature, chlorophyll *a* (Chl *a*) concentration, particle organic carbon (POC), particle organic nitrogen (PON), particle organic phosphorus (POP), NO_3, NO_2, Si, PO_4, and NH_4, and biological variables, including total bacteria abundance (bacterial abundance), total virus abundance (viral abundance), BP, and bacterial biomass production (BBP), were used to explore the relationship between microbial community function and the environment as well as the bacterial community activity.

DNA extraction and GeoChip hybridization

GeoChip is a comprehensive functional gene array for analyzing the functional diversity, composition, structure, metabolic potential/activity, and dynamics of microbial communities (Tu et al. 2014). GeoChip 4 contains ~ 82,000 probes covering 141,995 coding sequences from 410 functional gene families involved in carbon, nitrogen, phosphorus, and sulfur cycling, energy metabolism, antibiotic resistance, metal resistance/reduction, organic remediation, stress responses, bacteriophage, and virulence (Tu et al. 2014). In addition, the GeoChip provides the ability to analyze the functional gene families from all four microorganism domains, targeting a large number of archaea, bacterial, eukaryotic, and viral strains (Tu et al. 2014).

The DNA extraction protocol was described in the previous study (Zhang et al. 2013). The bacterioplankton community DNA from three representative pCO_2 mesocosms was applied for GeoChip hybridization. Briefly, DNA was isolated using the phenol/chloroform method accompanied by repeated freezing and thawing. Quantity and quality of DNA were measured by PicoGreen (Ahn et al. 1996) and NanoDrop, respectively. Then, 3 μg of DNA was labeled by Cy-3 and hybridized with GeoChip 4.0 on a Hybridization Station (MAUI, BioMicro Systems) at 42°C for 16 h (Tu et al. 2014). Hybridized DNA concentrations were measured by the PicoGreen method with a FLUOstar Optima (BMG Labtech).

GeoChip data processing and statistical analysis

The processing of GeoChip data was performed as described previously (Tu et al. 2014). Briefly, spots with a signal-to-noise ratio (SNR) < 2.0 were removed. Probe signal intensities were normalized by universal standards for GeoChip. To obtain reliable gene signal intensity, we only kept genes that were present in all three sampling mesocosms on the same sampling day, and we removed any genes that were present in less than three samples within each mesocosm. The Wilcoxon test was performed by the *base* package in R to evaluate the significant difference in signal intensity difference between each pair of two mesocosms. In addition, the repeated measure analysis of variance (ANOVA) was applied to test the influence of the pCO_2 on the gene signal intensity, and then paired sample *t*-test was performed to pairwise compare the signal intensity using the *base* package in R. To increase the accuracy, we focused on the genes that showed significant differences (the *p* value threshold for paired sample *t*-test and Wilcoxon test are 0.05 and 0.1, separately) in signal intensity comparison.

Furthermore, the linear correlation (Pearson's correlation) of gene signal intensity with the sampling day was conducted using the *base* package in R to evaluate the trends of gene signal intensity over time. Thereafter, further statistical analyses were conducted via the *vegan* package in R version 3.1.3 (R Development Core Team 2015), including (1) α diversity of functional gene structure (Shannon index and Pielou's evenness); (2) β diversity of community functional gene structure with Bray–Curtis dissimilarity, and the multivariate homogeneity of group dispersions (distance to the centroid of mesocosms) based on principal coordinates analysis; (3) detrended correspondence analysis (DCA) to illustrate the compositional differences of functional genes among three mesocosms during the experiment; (4) analysis of similarity (ANOSIM) to test the dissimilarity among the composition of bacterioplankton functional gene in three mesocosms; (5) redundancy analysis (RDA) to determine the relationship between environmental and biological variables (variance inflation factors > 20 were removed) and microbial functional gene community structure (pH, pCO_2, NO_2, NH_4, NO_3, temperature, BP, BBP, Chl *a*, and bacterial abundance were used as environmental and

biological variables); (6) Mantel tests to determine the major environmental and biological variables shaping microbial structure. The generalized linear regression was performed to test the influence of OA and experimental day on the diversity indexes of functional genes via *glmm* package in R. In addition, two-way ANOVA was used to test the influence of the OA (mesocosm) and gene category on the gene signal intensities. Correlation between functional genes and environmental and biological variables or experiment days was conducted by linear regression and Pearson's correlation via the *base* package in R.

Data availability

The EPOCA Svalbard 2010 mesocosm experiment dataset including over 50 parameters is available at Pangaea (doi: 10.1594/PANGAEA.769833). The GeoChip hybridization data are available at the website of the Institute of Environmental Genomics, University of Oklahoma (https://www.ou.edu/ieg/publications/datasets). The 16S rRNA gene raw sequences were deposited in the NCBI sequence reads archive with the number SRP092136.

Results

Characterization of mesocosms

With the addition of CO_2-enriched waters, the seawater pH of two mesocosms decreased to 7.74 and 7.51 in medium (M6) and high (M9) mesocosms, respectively, from days 1 to 4 until day 8–9 (Supporting Information Figs. S1, S2; Schulz et al. 2013). Then the pH of these two mesocosms increased to 7.89 and 7.72 on day 28, respectively, mostly driven by an interplay of air/sea gas exchange and biological consumption and production of CO_2 (Schulz et al. 2013). In the control mesocosms (M3), the pH was relatively stable throughout the experiment (8.34 ± 0.02). Here, three mesocosms (M3, M6, and M9) were chosen to represent control, medium, and high pCO_2 levels for GeoChip analysis. Salinity, temperature, and Chl *a* of three mesocosms showed a generally similar variation during the experiment (Supporting Information Fig. S2; Czerny et al. 2013; Riebesell et al. 2013; Schulz et al. 2013). The temperature increased from $\sim 2.5°C$ to $\sim 4°C$ from day 4 to day 7 and decreased by $\sim 1°C$ up to day 20, then increased sharply to $\sim 5.5°C$ on day 24. The Chl *a* increased during days 15–20 and days 25–30. The abundance of bacterioplankton decreased before day 6 and increased thereafter (Supporting Information Fig. S3). At the end of the experiment, the bacterioplankton population size in the low pCO_2 mesocosm was larger than that of those of the other two elevated pCO_2 mesocosms. Similar trends of BBP and BP were observed in the three mesocosms with an increase at the end of the experiment (Supporting Information Fig. S3). In addition, POC, PON, and POP showed significant differences between medium and high pCO_2 mesocosms compared with the under low pCO_2 (Schulz et al. 2013). Collectively, the elevated pCO_2 affected certain biological variables, such as primary production, BBP, BP, and particle organic matter that were associated with the bacterioplankton activity or mediated by bacterioplankton during the experiment (Riebesell et al. 2013).

Diversity and interaction of microbial functional genes

After removing low-quality and rare probes, a total of 6068 microbial function genes were detected by GeoChip 4 from 27,353 raw probes number in this study. The one-way ANOVA showed that the OA had a significant influence on Pielou's evenness instead of Shannon diversity ($F_{2,33} = 6.07$, $p = 0.006$ for Pielou's evenness and $F_{2,33} = 0.00$, $p = 1.000$ for Shannon diversity; Fig. 1a). Tukey's HSD analysis revealed significant differences in Pielou's evenness of control mesocosm compared to the other two treatment mesocosms (both $p < 0.05$). However, we did not find a significant difference in Pielou's evenness between medium-pCO_2 and high-pCO_2 mesocosms ($p = 0.848$). Further, the generalized linear regression of diversity indexes and experimental day showed that the OA had a significant influence on Pielou's evenness instead of Shannon diversity, while the experimental day showed a significant influence on Shannon diversity rather than Pielou's evenness (Supporting Information Table S1). These results suggested the influence of OA on the evenness rather than diversity of the microbial communities during our experiment. Generally, the value of Pielou's evenness was significantly correlated with the bacterial abundance, BP, and BBP (Fig. 1d; Pearson's product–moment correlation for bacterial abundance, $r = -0.48$, $p = 0.01$; for BP, $r = -0.41$, $p = 0.02$; for BBP, $r = -0.37$, $p = 0.04$), suggesting that the evenness changes might influence the activity and growth of the bacterioplankton community. In comparison, Shannon's diversity was significantly correlated with Chl *a* in the three mesocosms, indicating that the primary production changes by pCO_2 elevation affected the functional diversity of the microbial communities. The value of Pielou's evenness was also significantly correlated with the POC and PON (Fig. 1d; Pearson's product–moment correlation for POC, $r = -0.40$, $p = 0.02$; for PON, $r = -0.58$, $p < 0.01$). Moreover, Shannon's diversity was significantly correlated with the POC and POP (Pearson's product–moment correlation for POC, $r = -0.38$, $p = 0.03$; for POP, $r = -0.34$, $p = 0.04$). These results suggested the close relation of the diversity and evenness of functional genes with the phytoplankton and their generated particle organic matter.

The functional gene structures of bacterioplankton communities among different pCO_2 mesocosms were significantly dissimilar via the DCA (Fig. 1b) and ANOSIM test (statistic $R = 0.12$, $p = 0.018$). The average Bray–Curtis dissimilarity of the functional gene in the elevated mesocosms was lower than in the control mesocosm (paired sample *t*-test, control vs. medium, $p < 0.001$; control vs. high, $p = 0.001$; Supporting Information Fig. S4). Furthermore, the sparseness (distance to

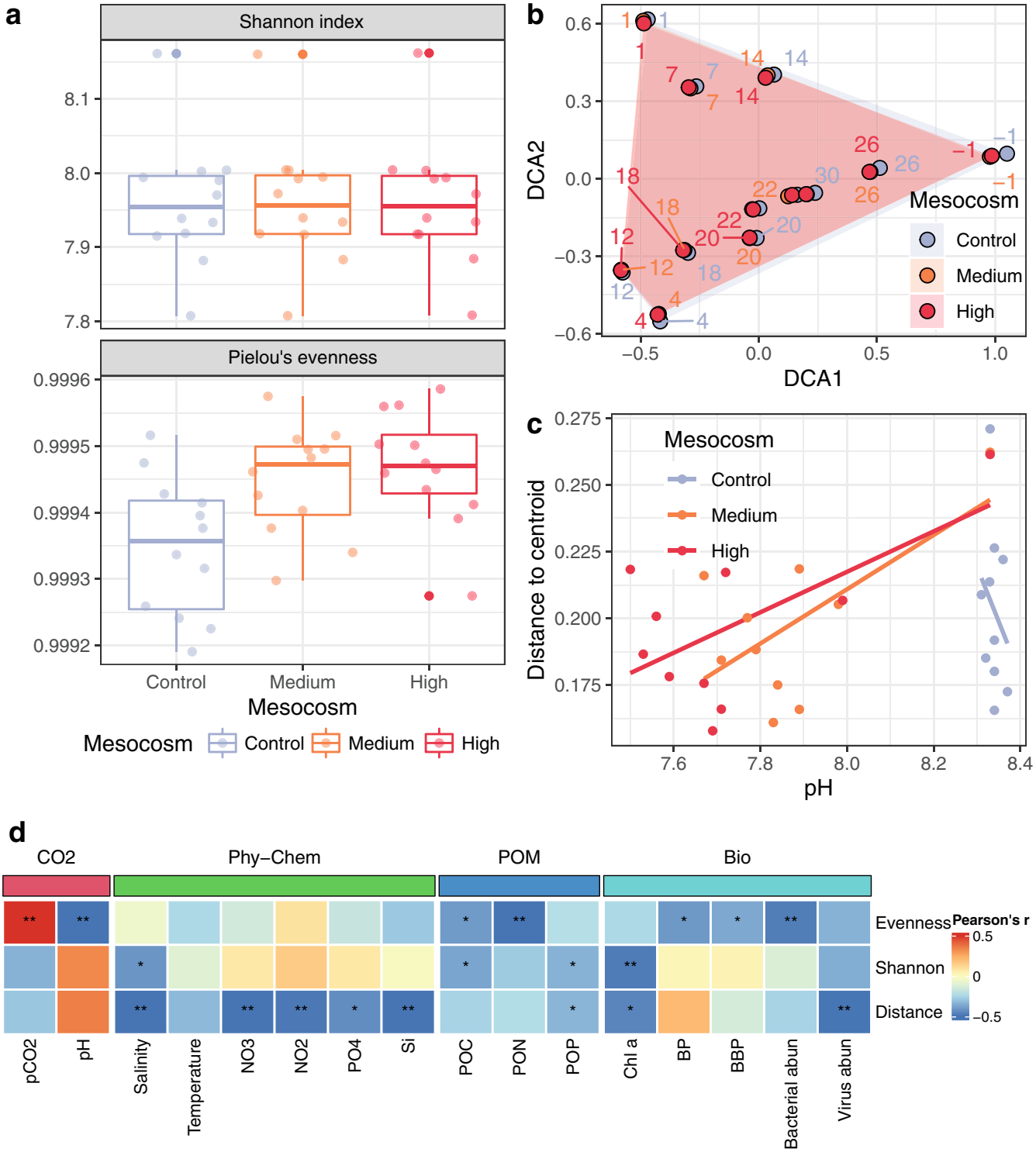

Fig. 1. Diversity of the functional genes and the correlation with the environmental and biological variables. (**a**) Changes in Shannon's diversity and Pielou's evenness during the sampling day. (**b**) Detrended correspondence analysis (DCA) based on the functional genes. The number indicates the sampling day. (**c**) Linear regression of the distance of each bacterioplankton community to the centroid and pH in each mesocosm (M3: $p > 0.05$; M6: $p < 0.05$; M9: $p < 0.05$). Distance to the centroid of each sample is based on principal coordinates analysis (PCoA). (**d**) Pearson's correlations of the diversity index and distance to centroid based on PCoA (Distance) with the environmental and biological variables. Bacterial abun: bacterial abundance; Virus abun: virus abundance. *$p < 0.05$; **$p < 0.01$.

the centroid) of the microbial functional community composition was positively correlated with the pH (Fig. 1c, Pearson's $r = 0.35$, $p = 0.05$), suggesting a lower variation in the functional gene structure under elevated pCO_2. These results indicated the increased similarity of the functional gene structure under elevated pCO_2.

To evaluate the response of microbial interactions to elevated pCO_2, we employed a molecular ecological network analysis using functional genes (Zhou et al. 2010) (Supporting Information Functional molecular ecological network construction and analysis). Generally, the complexity of functional microbial ecological networks (fMENs) increased with increasing pCO_2 (Supporting Information Table S2). The average clustering coefficient and average path distance increased with increasing pCO_2. Moreover, the relative modularity of fMEN increased in the high pCO_2 treatment. These results indicated that there were more complex connections of these functional genes under elevated pCO_2 conditions. Furthermore, the natural connectivity under elevated pCO_2 was greater than that under control pCO_2 after removing the same proportion of nodes (Supporting Information Fig. S5), indicating that the networks under elevated pCO_2 were more stable. Collectively, our results suggested that the elevated pCO_2 increased the complexity and stability of the functional gene network.

Functional genes of major biogeochemical processes

Two-way ANOVA results showed that the OA and gene category independently influenced the gene signal intensities (Supporting Information Table S3). Under different levels of pCO_2, several detected functional genes that are associated with carbon, nitrogen, and other biogeochemical cycling processes were altered in abundance (Supporting Information Fig. S6). Generally, the signal intensity of genes involved in biogeochemical cycling (e.g., carbon, nitrogen, and phosphorus cycling) was significantly higher in medium pCO_2 and high pCO_2 compared with control pCO_2 as revealed by repeated measure ANOVA and paired sample *t*-test (Supporting Information Fig. S7). However, only a few genes showed a significant difference among the mesocosms which was detected by the Wilcoxon test at 0.1 level (Fig. 2a). The following analysis, therefore, focused on these genes.

Four processes involved in carbon cycling were tested, including carbon degradation, carbon fixation, methane metabolism, and acetogenesis. We found that the normalized signal intensity of three genes associated with carbon degradation was significantly higher under elevated pCO_2 than one under control pCO_2 (at the 0.1 level), including endochitinase (chitin degradation), *lip* (lignin degradation), and *AssA* (other carbon degradation) (Fig. 2a). The related substrates were relatively recalcitrant. However, the genes involved in carbon fixation, including CODH, rubisco, *pcc*, and *aclB* gene, revealed nonsignificant differences among the three mesocosms. Three genes involved in methane metabolism were measured, including *pmoA* and *mmoX* for methane oxidation and *mcrA* for methane production. The signal intensity of *mmoX* was greater in elevated pCO_2 mesocosms than in the control pCO_2 mesocosm (Fig. 2a). The log ratio of means result showed that differences in the signal intensities of these genes under elevated pCO_2 compared to the control mesocosm were ranged (Fig. 2b,c).

Functional genes of all seven major processes associated with nitrogen cycling (ammonification, anammox, assimilatory nitrate/nitrite reduction, denitrification, dissimilatory nitrogen reduction, nitrification, and nitrogen fixation) were measured. The abundance of functional genes associated with nitrogen cycling was generally greater in elevated pCO_2 treatments than in the control pCO_2 treatment. However, we found that only four genes, including *nasA*, *nirA*, *NirB*, and *nifH*, revealed significantly greater normalized signal intensities in the elevated pCO_2 mesocosms than in the control pCO_2 mesocosm (Fig. 2a). The *nasA*, *nirA*, and *NirB* genes are involved in assimilatory nitrate reduction to ammonia, while the *nifH* gene is the key gene for nitrogen fixation. In addition, we found that the nifH and NirB genes positively correlated with experiment days in medium-pCO_2 mesocosm whereas no significant correlation with the day in the other two mesocosms (Supporting Information Fig. S8).

Three genes (*ppx*, phytase, and *ppk*) involved in phosphorus utilization were measured by GeoChip and none showed a significant difference among the treatments, although the signal intensities of these genes were greater under the elevated pCO_2 mesocosms (Fig. 2a). Six genes (*AprA*, APS_AprA, APS_AprB, *dsrA*, *dsrB*, and *sox*) associated with sulfur cycling were detected. Generally, the genes showed higher signal intensities under elevated pCO_2; however, only *AprB*, *dsrA*, and *dsrB* genes showed significant differences among the mesocosms (Fig. 2a). The *AprB* gene is involved in sulfate reduction to sulfite by encoding adenylyl-sulfate (adenosine-5′-phosphosulphate; APS) reductase. The *dsrA* and *dsrB* genes are the key genes for sulfite reduction to sulfide by encoding dissimilatory sulfite reductase. Furthermore, although the genes involved in phosphorus and sulfur cycling showed significantly negative correlations with the experimental day in the control pCO_2 mesocosm, no significant correlations were detected in the elevated pCO_2 mesocosms (Supporting Information Fig. S8). Therefore, the increase in these genes suggested that the elevated pCO_2 stimulated sulfate reduction and consequently increase sulfide.

Linkage of environmental variables to the functional traits of the bacterioplankton community

RDA revealed that about 48.2% of the variation in functional gene structure could be explained by the environmental and biological variables in our RDA model. The RDA results also showed that both physicochemical (e.g., temperature, pH, and NO_3) and biological (e.g., BP, BBP, and Chl *a*) variables strongly affected the microbial functional gene community structure (Fig. 3a). The Mantel test results showed that the changes in pH and pCO_2 strongly influenced the functional gene structure under elevated

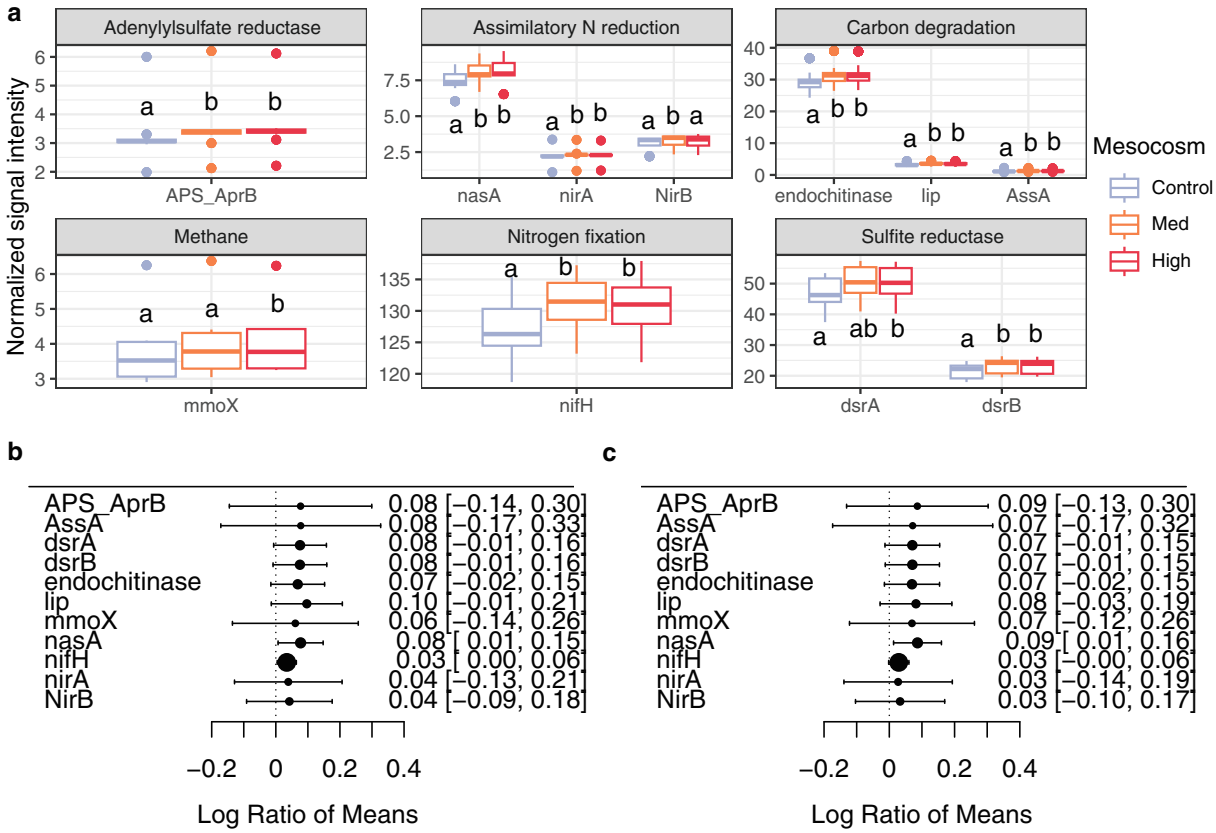

Fig. 2. Normalized signal intensity and the log ratio of means of detected key genes involved in carbon, nitrogen, phosphorus, and sulfur cycling. (**a**) The signal intensity for each functional gene category is the average total signal intensity from all samples in each mesocosm. Only the genes that had a significant difference between mesocosms were shown. The APS_AprB gene encodes adenylyl-sulfate (adenosine-5′-phosphosulphate, APS) reductase, which is involved in sulfate reduction. The *nasA*, *nirA*, and *NirB* genes encode nitrate transporter, ferredoxin-nitrite reductase, and nitrite reductase (NADH) large subunit, separately, which are involved in assimilatory nitrate reduction to ammonia. Endochitinase is involved in chitin degradation. The *lip* gene encodes triacylglycerol lipase, which is involved in lignin degradation. The *AssA* gene encodes archaetidylserine synthase, which is involved in other carbon degradation. The *mmoX* gene encodes methane monooxygenase component A, which is involved in methane oxidation. The *nifH* gene encodes nitrogenase, which is the key gene for nitrogen fixation. The *dsrA* and *dsrB* genes encode dissimilatory sulfite reductase, which is involved in sulfite reduction to sulfide. Letter a and b represented the significance with a $p < 0.10$ as tested by the Wilcoxon test. All data are presented as mean ± SD. (**b**) Log ratio of means in comparison between control and medium pCO_2 mesocosms. (**c**) Log ratio of means in comparison between control and high pCO_2 mesocosms.

pCO_2 (Fig. 3b–d). We also found that the functional gene structure variation had a strong relationship with the BP under elevated pCO_2, suggesting the close relation of functional gene structure with BP under pCO_2 changes. The Mantel test results showed that the BP showed a significant correlation with the structure of functional genes under elevated pCO_2, while no significant correlation was detected under control pCO_2 (Fig. 3b–d). Collectively, these results suggested that the elevated pCO_2 may have altered the relationship between the functional structure of bacterioplankton and community functioning.

Discussion

OA altered microbial functional diversity

Understanding the response of the bacterial community to OA is a vital issue for evaluating the anthropogenic influence on the ocean (Cavicchioli et al. 2019). As one of the largest OA mesocosm experiments, the EPOCA Svalbard experiment provided a unique opportunity to do so (Quirin 2011; Riebesell et al. 2013). The negligible difference in microbial phylogenetic diversity among the different pCO_2 treatments was demonstrated by the 16S rRNA gene during the EPOCA experiment (Roy et al. 2013; Zhang et al. 2013; Wang et al. 2016). Similarly, we found that the functional gene Shannon index changes of bacterioplankton communities under the elevated pCO_2 showed an insignificant response to OA. However, the beta diversity (Bray–Curtis dissimilarity) decreased along with the decreased pH (Fig. 1). This indicates that more functional groups/species are lost under elevated pCO_2. This may be related to the increase in selection for specific metabolic pathways caused by the disturbance of increased pCO_2 (known as the "metabolic niche effect" or "environmental filtering") (Louca et al. 2016). In addition, the

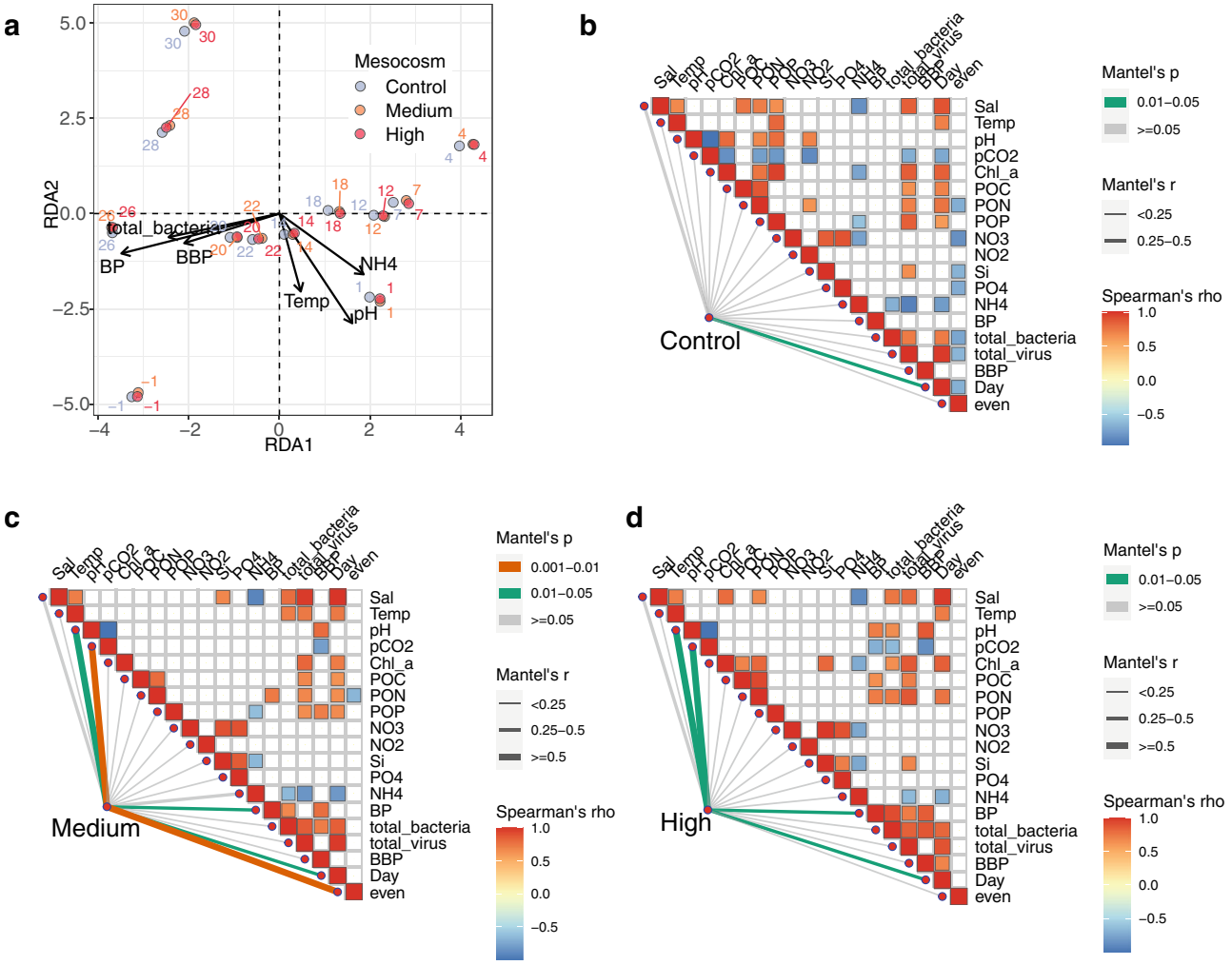

Fig. 3. Relationship between functional gene structure and the environmental and biological variables. (**a**) Redundancy analysis (RDA) is based on the functional gene structure and environmental and biological variables. The number indicates the sampling day. (**b–d**) Correlations of the functional gene structure (Bray–Curtis dissimilarity) in control (M3, **b**), medium (M6, **c**), and high (M9, **d**) pCO_2 mesocosms with the environmental and biological variables and day. The edge width indicates Mantel's *r* value and the edge color denotes statistical significance. Pairwise correlations of these variables are shown with a color gradient denoting Spearman's correlation coefficient. Environmental and biological variables include salinity (Sal), temperature (Temp), pH, pCO_2, chlorophyll *a* (Chl *a*), particle organic carbon (POC), particle organic nitrogen (PON), particle organic phosphorus (POP), nitrate (NO_3), nitrite (NO_2), ammonium (NH_4), bacterial production (BP), bacterial biomass production (BBP), bacterial abundance (total_bacteria), viral abundance (total_virus).

lower dissimilarity of functional gene structure under elevated pCO_2 suggested that the medium-pCO_2 and high-pCO_2 groups reached a more stable community composition over time (Supporting Information Fig. S4). This is consistent with a previous study of an embayment in Norway showing that the elevated pCO_2 decreased the phylogenetic turnover rate (Oliver et al. 2014). Furthermore, functional gene molecular ecological network analysis revealed a more complex interaction as well as higher stability under medium-pCO_2 and high-pCO_2 compared with control-pCO_2 (Supporting Information Fig. S5; Table S2). This is probably because OA acts as a deterministic filtering factor to select certain bacterioplankton (Roy et al. 2013; Zhang et al. 2013; Wang et al. 2016), and this could further trigger a series of dynamic changes among different microorganisms. The increased stability along with increased complexity is in accordance with the patterns observed in macroecology (Montoya et al. 2006), supporting MacArthur's argument that the complexity of ecosystems begets their stability (MacArthur 1955). Decreased pH enhancing the stability and complexity of the microbial community network was also found in a soil environment (Yang et al. 2022). A previous study suggested that microbial ecological network complexity and stability appeared to be more tightly associated with the microbial community functional

structure and ecosystem functional processes under climate warming (Yuan et al. 2021). Since changes in ecosystem function may result from disruptions in biological interactions (Doney et al. 2012), our results suggest that the microbial ecosystem function of the Arctic Ocean could be altered by high pCO_2 via altered interaction among microbial functional groups.

Biodiversity is usually correlated with production in the ecosystem, and thus changes in biodiversity influence the ecosystem functioning (Hooper et al. 2005; Cardinale et al. 2012; Hooper et al. 2012). Generally, negative correlations of BP and BBP with evenness were observed in the current study (Fig. 1d). Moreover, we found close relationships between functional gene structures and BP, especially under elevated pCO_2 (Fig. 3). These results indicate that the diversity of functional genes and the complexity of their interactions are tightly associated with the production of bacterioplankton. Furthermore, the negative correlations indicate that the increased functional gene evenness and complexity induce decreased productivity caused by the increased pCO_2. Under high pCO_2 and low pH environments, bacterioplankton have to use more energy for regulating intracellular pH balance (Hopkinson et al. 2010). To be successful competitors, bacterioplankton might sacrifice some of their potential production for adapting to the environmental changes induced by elevated pCO_2. Therefore, our results suggest that the bacterioplankton community seemed to be less productive under OA. A previous study documented that OA positively affected the genes related to carbon and nitrogen cycling in a low-latitude warm ocean (Xia et al. 2019), but it is unclear whether OA-induced network changes will affect ecosystem functional processes. Our analysis further suggested that the OA-affected network complexity and stability appeared to be associated with bacterioplankton production, and this finding highlighted the important influence of elevated pCO_2 on the BP-diversity pattern and even the entire ecosystem.

Response of genes involved in biogeochemical cycling to elevated pCO_2

The N_2-fixation by diazotrophs is the major way for new nitrogen to be introduced into the ocean from the atmosphere and is one of the processes that are more susceptible to pCO_2 changes (Wannicke et al. 2018). The elevated pCO_2 increased the efficiency of carbon concentrating mechanisms of diazotrophs during cyanobacterial photosynthesis, in turn increasing the availability of energic resources and stimulating the growth and N_2-fixation of diazotrophs (Kranz et al. 2009, 2010). Consistent with this, we observed a higher abundance of the *nifH* gene during the experiment under medium- and high-pCO_2 concentrations (Fig. 2), suggesting an increased potential for N_2-fixation. We also found a significantly positive correlation between the *nifH* gene and experimental day under medium-pCO_2 concentration (Supporting Information Fig. S8), which suggested the possible influence of OA on this process. The significantly positive correlation between NH_4^+ concentration and total *nifH* gene abundance (Supporting Information Fig. S9; Pearson's correlation $r = 0.34$, $p = 0.04$) highlights the important role of bacterial diazotrophs. Nitrogen fixation was closely related to methane oxidization in an acidic peat ecosystem (Liebner and Svenning 2013). We found higher signal intensities of a methane oxidization gene (*mmoX*) under elevated pCO_2 compared with control pCO_2. This result highlights the potential coupling of methane oxidization and nitrogen fixation and illustrated the importance of methane-oxidizing bacteria under elevated pCO_2. In addition to N_2 fixation, assimilatory nitrate/nitrite reduction is another contributor to NH_4^+ from NO_3^-. Three different nitrate-reducing systems have been described in microbes, i.e., assimilatory nitrate reductases (Nas), membrane-bounded nitrate reductases (Nar), and periplasmic dissimilatory reductases (Nap) (Moreno-Vivián et al. 1999; Richardson 2000; Richardson et al. 2001; Lledó et al. 2005). The components of the Nas system were higher under elevated pCO_2 than control pCO_2, including the *nasA*, *nirA*, and *NirB* genes (Fig. 2), suggesting an increase in assimilatory nitrate/nitrite reduction. This is possibly associated with the decreased nitrification that increased the competition in the usage of NO_3^- under the decreased pH environment.

The changes in POC and DOC concentrations, as well as the fatty acid composition (Czerny et al. 2013; Engel et al. 2013; Leu et al. 2013), indicate that the changes in the substrate for heterotrophic bacteria enhanced the release of DOC during autotrophic production at high pCO_2 as the result of heterotrophic activity (Engel et al. 2013). We observed significant changes in the genes involved in carbon degradation under elevated pCO_2, including chitin and lignin degradation (Fig. 2). In addition, the exochitinase significantly increased over experimental days under elevated pCO_2 whereas decreased under control pCO_2 (Supporting Information Fig. S8). The activities of bacterial protease, α-glucosidase, and β-glucosidase were the highest at elevated pCO_2 levels during the experiment (Grossart et al. 2006). Similarly, microbial polysaccharide degradation can be stimulated under acidification conditions (Piontek et al. 2010). We found that the signal intensities of endochitinase, *lip*, and *AssA* genes were significantly correlated with POC (Supporting Information Fig. S10). In addition, the close relationship between BP and the carbon cycling gene profile is useful for inferring microbial function. This is supported by the significant correlation between BP and functional gene structure under elevated pCO_2 (Fig. 3). Although the changes in pCO_2 potentially influenced BP, growth rate, and growth balance than the conversion of dissolved organic matter into CO_2 (Motegi et al. 2013), the functional gene profile changes might affect the function of microbial communities on a long timescale, as in soil environments (He et al. 2010). Moreover, a lower correlation of Chl *a* to particulate organic nitrogen under elevated pCO_2 suggested that higher amounts of nutrients were

partitioned into the heterotrophic food web (Engel et al. 2013), a process that might profit the carbon degradation of bacterioplankton. The abundance of genes involved in the recalcitrant carbon degradation changed under elevated pCO_2, indicating that the stock of organic carbon may be affected in the long term.

The dimethylsulfoniopropionate (DMSP) generation was increased by the elevated pCO_2, since the major DMSP producers, dinoflagellates, were stimulated (Archer et al. 2013). The significant correlation between BP and the DMS:DMSP ratio indicated the regulatory role of bacteria on DMS concentration under elevated pCO_2 (Archer et al. 2013). Here, we found several genes involved in sulfur metabolism significantly correlated with BP or BBP, including the APS_AprA, *sox*, *dsrA*, and *dsrB* genes (Supporting Information Fig. S11). This result indicates the active role of the bacteria in marine sulfur cycling. In addition, we found that the elevated pCO_2 increased the signal intensity of the genes involved in sulfide and sulfate reduction (Fig. 2). These results suggest that more sulfites would be generated under elevated pCO_2 since these two pathways mediate the transformation of sulfide and sulfate to sulfite. Collectively, our results indicate that the OA significantly affects the sulfur metabolism mediated by bacteria. Unfortunately, GeoChip 4.0 did not contain other genes involved in sulfur cycling. Thus, our study emphasizes the need to investigate the OA effect on the sulfur cycling mediated by bacteria in future studies.

Conclusion

Although the phylogenetic diversity was shown to not be susceptible to OA during the EPOCA experiment (Roy et al. 2013; Zhang et al. 2013), the elevated pCO_2 and decreased pH significantly altered the functional gene structure and evenness of the bacterioplankton community in the Arctic Ocean. Despite the only moderate duration of this experiment, significant changes in functional gene structure and evenness were detected, implying the possible disputation by elevated pCO_2 to the function of bacterial communities (Supporting Information Consideration of the mesocosm experiment). In addition, the OA resulted in a stable bacterioplankton community structure with relatively complex interactions. The close relationships between the structure and diversity of the bacterioplankton communities and their production indicated that the OA would shift the functional gene structure and consequently the role of the bacterioplankton community in the biogeochemical cycling in the Arctic Ocean. Our results also indicated specific responses of the bacterioplankton community involved in carbon degradation, nitrogen fixation, assimilatory nitrate/nitrite reduction, adenyl sulfate redaction, and sulfur reduction to elevated pCO_2. These changes would affect the oceanic food webs, fisheries, and carbon export to the deep sea (Yool et al. 2007; Beman et al. 2011).

References

Ahn, S. J., J. Costa, and J. R. Emanuel. 1996. PicoGreen quantitation of DNA: Effective evaluation of samples pre- or post-PCR. Nucleic Acids Res. **24**: 2623–2625. doi:10.1093/nar/24.13.2623

Archer, S. D., S. A. Kimmance, J. A. Stephens, F. E. Hopkins, R. G. J. Bellerby, K. G. Schulz, J. Piontek, and A. Engel. 2013. Contrasting responses of DMS and DMSP to ocean acidification in Arctic waters. Biogeosciences **10**: 1893–1908. doi:10.5194/bg-10-1893-2013

Azam, F., and F. Malfatti. 2007. Microbial structuring of marine ecosystems. Nat. Rev. Microbiol. **5**: 782–791. doi:10.1038/nrmicro1747

Azam, F., T. Fenchel, J. G. Field, J. S. Gray, L. A. Meyerreil, and F. Thingstad. 1983. The ecological role of water-column microbes in the sea. Mar. Ecol. Prog. Ser. **10**: 257–263. doi:10.3354/meps010257

Bellerby, R. G. J., A. Silyakova, G. Nondal, D. Slagstad, J. Czerny, T. de Lange, and A. Ludwig. 2012. Marine carbonate system evolution during the EPOCA Arctic pelagic ecosystem experiment in the context of simulated Arctic Ocean acidification. Biogeosci. Discuss. **9**: 15541–15565. doi:10.5194/bgd-9-15541-2012

Beman, J. M., and others. 2011. Global declines in oceanic nitrification rates as a consequence of ocean acidification. Proc. Natl. Acad. Sci. USA **108**: 208–213. doi:10.1073/pnas.1011053108

Brussaard, C. P. D., A. A. M. Noordeloos, H. Witte, M. C. J. Collenteur, K. Schulz, A. Ludwig, and U. Riebesell. 2013. Arctic microbial community dynamics influenced by elevated CO_2 levels. Biogeosciences **10**: 719–731. doi:10.5194/bg-10-719-2013

Caldeira, K., and M. E. Wickett. 2005. Ocean model predictions of chemistry changes from carbon dioxide emissions to the atmosphere and ocean. J. Geophys. Res.: Oceans **110**: C09S04. doi:10.1029/2004JC002671

Cardinale, B. J., and others. 2012. Biodiversity loss and its impact on humanity. Nature **486**: 59–67. doi:10.1038/nature11148

Cavicchioli, R., and others. 2019. Scientists' warning to humanity: Microorganisms and climate change. Nat. Rev. Microbiol. **17**: 569–586. doi:10.1038/s41579-019-0222-5

Crawfurd, K. J., S. Alvarez-Fernandez, K. D. A. Mojica, U. Riebesell, and C. P. D. Brussaard. 2017. Alterations in microbial community composition with increasing fCO_2: A mesocosm study in the eastern Baltic Sea. Biogeosciences **14**: 3831–3849. doi:10.5194/bg-14-3831-2017

Czerny, J., and others. 2013. Implications of elevated CO_2 on pelagic carbon fluxes in an Arctic mesocosm study—An elemental mass balance approach. Biogeosciences **10**: 3109–3125. doi:10.5194/bg-10-3109-2013

Deppeler, S., K. Petrou, K. G. Schulz, K. Westwood, I. Pearce, J. McKinlay, and A. Davidson. 2018. Ocean acidification of a

coastal Antarctic marine microbial community reveals a critical threshold for CO_2 tolerance in phytoplankton productivity. Biogeosciences **15**: 209–231. doi:10.5194/bg-15-209-2018

Doney, S. C., V. J. Fabry, R. A. Feely, and J. A. Kleypas. 2009. Ocean acidification: The other CO_2 problem. Ann. Rev. Mar. Sci. **1**: 169–192. doi:10.1146/annurev.marine.010908.163834

Doney, S. C., and others. 2012. Climate change impacts on marine ecosystems. Ann. Rev. Mar. Sci. **4**: 11–37. doi:10.1146/annurev-marine-041911-111611

Dutkiewicz, S., J. J. Morris, M. J. Follows, J. Scott, O. Levitan, S. T. Dyhrman, and I. Berman-Frank. 2015. Impact of ocean acidification on the structure of future phytoplankton communities. Nat. Clim. Change **5**: 1002–1006. doi:10.1038/nclimate2722

Eberlein, T., S. Wohlrab, B. Rost, U. John, L. T. Bach, U. Riebesell, and D. B. Van de Waal. 2017. Effects of ocean acidification on primary production in a coastal North Sea phytoplankton community. PLoS ONE **12**: e0172594. doi:10.1371/journal.pone.0172594

Ekstrom, J. A., and others. 2015. Vulnerability and adaptation of US shellfisheries to ocean acidification. Nat. Clim. Change **5**: 207–214. doi:10.1038/nclimate2508

Engel, A., C. Borchard, J. Piontek, K. G. Schulz, U. Riebesell, and R. Bellerby. 2013. CO_2 increases ^{14}C primary production in an Arctic plankton community. Biogeosciences **10**: 1291–1308. doi:10.5194/bg-10-1291-2013

Falkowski, P. G., R. T. Barber, and V. V. Smetacek. 1998. Biogeochemical controls and feedbacks on ocean primary production. Science **281**: 200–207. doi:10.1126/science.281.5374.200

Fantazzini, P., and others. 2015. Gains and losses of coral skeletal porosity changes with ocean acidification acclimation. Nat. Commun. **6**: 7785. doi:10.1038/ncomms8785

Fuhrman, J. A. 1999. Marine viruses and their biogeochemical and ecological effects. Nature **399**: 541–548. doi:10.1038/21119

Grossart, H.-P., M. Allgaier, U. Passow, and U. Riebesell. 2006. Testing the effect of CO_2 concentration on the dynamics of marine heterotrophic bacterioplankton. Limnol. Oceanogr. **51**: 1–11. doi:10.4319/lo.2006.51.1.0001

He, Z., and others. 2010. Metagenomic analysis reveals a marked divergence in the structure of belowground microbial communities at elevated CO_2. Ecol. Lett. **13**: 564–575. doi:10.1111/j.1461-0248.2010.01453.x

Hofmann, G. E., J. P. Barry, P. J. Edmunds, R. D. Gates, D. A. Hutchins, T. Klinger, and M. A. Sewell. 2010. The effect of ocean acidification on calcifying organisms in marine ecosystems: An organism-to-ecosystem perspective. Annu. Rev. Ecol. Evol. Syst. **41**: 127–147. doi:10.1146/annurev.ecolsys.110308.120227

Hooper, D. U., and others. 2005. Effects of biodiversity on ecosystem functioning: A consensus of current knowledge. Ecol. Monogr. **75**: 3–35. doi:10.1890/04-0922

Hooper, D. U., and others. 2012. A global synthesis reveals biodiversity loss as a major driver of ecosystem change. Nature **486**: 105–108. doi:10.1038/nature11118

Hopkinson, B. M., Y. Xu, D. Shi, P. J. McGinn, and F. M. M. Morel. 2010. The effect of CO_2 on the photosynthetic physiology of phytoplankton in the Gulf of Alaska. Limnol. Oceanogr. **55**: 2011–2024. doi:10.4319/lo.2010.55.5.2011

IPCC. 2015. IPCC, 2014: Climate change 2014: Synthesis report. Contribution of working groups I, II and III to the fifth assessment report of the intergovernmental panel on climate change. IPCC.

Jiao, N., and others. 2010. Microbial production of recalcitrant dissolved organic matter: Long-term carbon storage in the global ocean. Nat. Rev. Microbiol. **8**: 593–599. doi:10.1038/nrmicro2386

Joint, I., S. C. Doney, and D. M. Karl. 2011. Will ocean acidification affect marine microbes? ISME J. **5**: 1–7. doi:10.1038/ismej.2010.79

van Kessel, M. A., D. R. Speth, M. Albertsen, P. H. Nielsen, H. J. M. Op den Camp, B. Kartal, M. S. M. Jetten, and S. Lücker. 2015. Complete nitrification by a single microorganism. Nature **528**: 555–559. doi:10.1038/nature16459

Kranz, S. A., D. Sültemeyer, K.-U. Richter, and B. Rost. 2009. Carbon acquisition by Trichodesmium: The effect of pCO_2 and diurnal changes. Limnol. Oceanogr. **54**: 548–559. doi:10.4319/lo.2009.54.2.0548

Kranz, S. A., O. Levitan, K. U. Richter, O. Prasil, I. Berman-Frank, and B. Rost. 2010. Combined effects of CO_2 and light on the N_2-fixing cyanobacterium Trichodesmium IMS101: Physiological responses. Plant Physiol. **154**: 334–345. doi:10.1104/pp.110.159145

Leu, E., M. Daase, K. G. Schulz, A. Stuhr, and U. Riebesell. 2013. Effect of ocean acidification on the fatty acid composition of a natural plankton community. Biogeosciences **10**: 1143–1153. doi:10.5194/bg-10-1143-2013

Liebner, S., and M. M. Svenning. 2013. Environmental transcription of *mmoX* by methane-oxidizing *Proteobacteria* in a subarctic Palsa peatland. Appl. Environ. Microbiol. **79**: 701–706. doi:10.1128/AEM.02292-12

Lledó, B., F. C. Marhuenda-Egea, R. Martínez-Espinosa, and M. Bonete. 2005. Identification and transcriptional analysis of nitrate assimilation genes in the halophilic archaeon *Haloferax mediterranei*. Gene **361**: 80–88. doi:10.1016/j.gene.2005.07.011

Louca, S., L. W. Parfrey, and M. Doebeli. 2016. Decoupling function and taxonomy in the global ocean microbiome. Science **353**: 1272–1277. doi:10.1126/science.aaf4507

Maas, E. W., C. S. Law, J. A. Hall, S. Pickmere, K. I. Currie, F. H. Chang, K. Matt Voyles, and D. Caird. 2013. Effect of ocean acidification on bacterial abundance, activity and diversity in the Ross Sea, Antarctica. Aquat. Microb. Ecol. **70**: 1–15. doi:10.3354/ame01633

MacArthur, R. 1955. Fluctuations of animal populations and a measure of community stability. Ecology **36**: 533–536. doi:10.2307/1929601

Monier, A., H. S. Findlay, S. Charvet, and C. Lovejoy. 2014. Late winter under ice pelagic microbial communities in the high Arctic Ocean and the impact of short-term exposure to elevated CO_2 levels. Front. Microbiol. **5**: 490. doi:10.3389/fmicb.2014.00490

Montoya, J. M., S. L. Pimm, and R. V. Solé. 2006. Ecological networks and their fragility. Nature **442**: 259–264. doi:10.1038/nature04927

Moreno-Vivián, C., P. Cabello, M. Martínez-Luque, R. Blasco, and F. Castillo. 1999. Prokaryotic nitrate reduction: Molecular properties and functional distinction among bacterial nitrate reductases. J. Bacteriol. **181**: 6573–6584. doi:10.1128/JB.181.21.6573-6584.1999

Motegi, C., T. Tanaka, J. Piontek, C. P. D. Brussaard, J. P. Gattuso, and M. G. Weinbauer. 2013. Effect of CO_2 enrichment on bacterial metabolism in an Arctic fjord. Biogeosciences **10**: 3285–3296. doi:10.5194/bg-10-3285-2013

Newbold, L. K., and others. 2012. The response of marine picoplankton to ocean acidification. Environ. Microbiol. **14**: 2293–2307. doi:10.1111/j.1462-2920.2012.02762.x

Oliver, A. E., L. K. Newbold, A. S. Whiteley, and C. J. van der Gast. 2014. Marine bacterial communities are resistant to elevated carbon dioxide levels. Environ. Microbiol. Rep. **6**: 574–582. doi:10.1111/1758-2229.12159

Piontek, J., M. Lunau, N. Handel, C. Borchard, M. Wurst, and A. Engel. 2010. Acidification increases microbial polysaccharide degradation in the ocean. Biogeosciences **7**: 1615–1624. doi:10.5194/bg-7-1615-2010

Piontek, J., C. Borchard, M. Sperling, K. G. Schulz, U. Riebesell, and A. Engel. 2013. Response of bacterioplankton activity in an Arctic fjord system to elevated pCO_2: Results from a mesocosm perturbation study. Biogeosciences **10**: 297–314. doi:10.5194/bg-10-297-2013

Quéré, L. C., and others. 2013. Global carbon budget 2013. Earth Syst. Sci. Data Discuss. **6**: 689–760.

Quirin, S. 2011. Environment: Earth's acid test. Nat. News **471**: 154–156. doi:10.1038/471154a

R Development Core Team. 2015. R: A language and environment for statistical computing. R Foundation for Statistical Computing.

Raven, J., and others. 2005. Ocean acidification due to increasing atmospheric carbon dioxide. The Royal Society.

Richardson, D. J. 2000. Bacterial respiration: A flexible process for a changing environment. Microbiology **146**: 551–571. doi:10.1099/00221287-146-3-551

Richardson, D. J., B. C. Berks, D. A. Russell, S. Spiro, and C. J. Taylor. 2001. Functional, biochemical and genetic diversity of prokaryotic nitrate reductases. Cell. Mol. Life Sci. **58**: 165–178. doi:10.1007/PL00000845

Riebesell, U., J. P. Gattuso, T. F. Thingstad, and J. J. Middelburg. 2013. Preface "Arctic Ocean acidification: Pelagic ecosystem and biogeochemical responses during a mesocosm study". Biogeosciences **10**: 5619–5626. doi:10.5194/bg-10-5619-2013

Robinson, C. J., B. J. M. Bohannan, and V. B. Young. 2010. From structure to function: The ecology of host-associated microbial communities. Microbiol. Mol. Biol. Rev. **74**: 453–476.

Roy, A. S., and others. 2013. Ocean acidification shows negligible impacts on high-latitude bacterial community structure in coastal pelagic mesocosms. Biogeosciences **10**: 555–566. doi:10.5194/bg-10-555-2013

Schulz, K. G., and others. 2013. Temporal biomass dynamics of an Arctic plankton bloom in response to increasing levels of atmospheric carbon dioxide. Biogeosciences **10**: 161–180. doi:10.5194/bg-10-161-2013

Tu, Q., and others. 2014. GeoChip 4: A functional gene-array-based high-throughput environmental technology for microbial community analysis. Mol. Ecol. Resour. **14**: 914–928. doi:10.1111/1755-0998.12239

Turk-Kubo, K. A., M. Karamchandani, D. G. Capone, and J. P. Zehr. 2014. The paradox of marine heterotrophic nitrogen fixation: Abundances of heterotrophic diazotrophs do not account for nitrogen fixation rates in the eastern tropical South Pacific. Environ. Microbiol. **16**: 3095–3114. doi:10.1111/1462-2920.12346

Wang, Y., R. Zhang, Q. Zheng, Y. Deng, J. D. Van Nostrand, J. Zhou, and N. Jiao. 2016. Bacterioplankton community resilience to ocean acidification: Evidence from microbial network analysis. ICES J. Mar. Sci. **73**: 865–875. doi:10.1093/icesjms/fsv187

Wannicke, N., C. Frey, C. S. Law, and M. Voss. 2018. The response of the marine nitrogen cycle to ocean acidification. Glob. Change Biol. **24**: 5031–5043. doi:10.1111/gcb.14424

Ward, B. B., A. H. Devol, J. J. Rich, B. X. Chang, S. E. Bulow, H. Naik, A. Pratihary, and A. Jayakumar. 2009. Denitrification as the dominant nitrogen loss process in the Arabian Sea. Nature **461**: 78–81. doi:10.1038/nature08276

Westwood, K. J., P. G. Thomson, R. L. van den Enden, L. E. Maher, S. W. Wright, and A. T. Davidson. 2018. Ocean acidification impacts primary and bacterial production in Antarctic coastal waters during austral summer. J. Exp. Mar. Biol. Ecol. **498**: 46–60. doi:10.1016/j.jembe.2017.11.003

Whitman, W. B., D. C. Coleman, and W. J. Wiebe. 1998. Prokaryotes: The unseen majority. Proc. Natl. Acad. Sci. USA **95**: 6578–6583. doi:10.1073/pnas.95.12.6578

Xia, X., Y. Wang, Y. Yang, T. Luo, J. D. Van Nostrand, J. Zhou, N. Jiao, and R. Zhang. 2019. Ocean acidification regulates the activity, community structure, and functional potential of heterotrophic bacterioplankton in an oligotrophic gyre. J. Geophys. Res.: Biogeosciences **124**: 1001–1017. doi:10.1029/2018JG004707

Yang, Y., Y. Shi, J. Fang, H. Chu, and J. M. Adams. 2022. Soil microbial network complexity varies with pH as a

continuum, not a threshold, across the North China plain. Front. Microbiol. **13**: 895687. doi:10.3389/fmicb.2022.895687

Yool, A., A. P. Martin, C. Fernández, and D. R. Clark. 2007. The significance of nitrification for oceanic new production. Nature **447**: 999–1002. doi:10.1038/nature05885

Yuan, M. M., and others. 2021. Climate warming enhances microbial network complexity and stability. Nat Clim Change **11**: 343–348. doi:10.1038/s41558-021-00989-9

Zhang, R., X. Xia, S. C. K. Lau, C. Motegi, M. G. Weinbauer, and N. Jiao. 2013. Response of bacterioplankton community structure to an artificial gradient of pCO_2 in the Arctic Ocean. Biogeosciences **10**: 3679–3689. doi:10.5194/bg-10-3679-2013

Zhou, J., Y. Deng, F. Luo, Z. He, Q. Tu, and X. Zhi. 2010. Functional molecular ecological networks. mBio **1**: e00169-10. doi:10.1128/mBio.00169-10

Zhou, G., and others. 2016. Changes in microbial communities, photosynthesis and calcification of the coral *Acropora gemmifera* in response to ocean acidification. Sci. Rep. **6**: 35971. doi:10.1038/srep35971

Acknowledgment

This work was supported by the National Key R&D Program Intergovernmental Key Special Project (2021YFE0193000) and NSFC (42188102, 41861144018). This work contributes to the European Project on Ocean Acidification (EPOCA, FP7 contract #211384). We gratefully acknowledge Greenpeace International for assistance with the transport of the mesocosm facility from Kiel to Ny-Ålesund and back. We also thank the captains and crews of M/V ESPERANZA (Greenpeace) and R/V Viking Explorer (University Centre in Svalbard [UNIS]) for assistance during mesocosm transport, deployment, and recovery in Kongsfjord. We thank Tong Yuan, Caiyun Yang, and Feifei Liu for their GeoChip technological assistance during this study.

Conflict of Interest

None declare.

Submitted 16 February 2022
Revised 22 September 2022
Accepted 06 May 2023

Deputy editor: C. Elisa Schaum